

1 Carbon balance and emissions of methane and nitrous oxide during 2 four years of moderate rewetting of a cultivated peat soil site 3

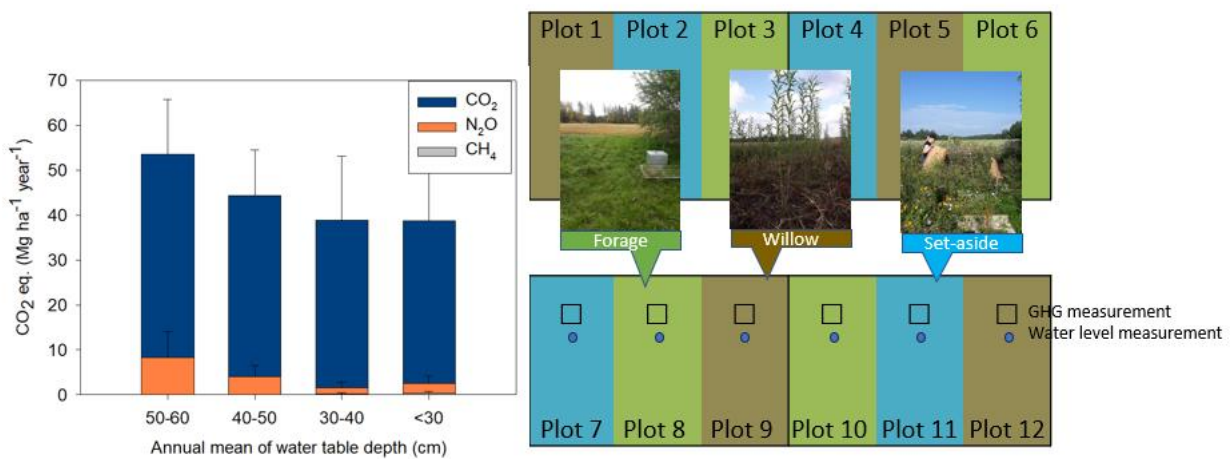
4 Kristiina Lång*, Henri Honkanen, Jaakko Heikkinen, Sanna Saarnio, Tuula Larmola, Hanna Kekkonen
5 Natural Resources Institute Finland, Latokartanonkaari 9, FI-00790 Helsinki, Finland

6 *Correspondence to:* Kristiina Lång (kristiina.lang@luke.fi)
7

8 **Abstract.** Raising the water table is an effective way to abate greenhouse gas emissions from cultivated peat soils. We
9 experimented a gradual water table rise at a highly degraded agricultural peat soil site with plots of willow, forage and mixed
10 vegetation (set-aside) in southern Finland. We measured the emissions of carbon dioxide (CO₂), methane (CH₄) and nitrous
11 oxide (N₂O) for four years. The mean annual ground water table depth was about 80, 40, 40 and 30 cm in 2019-2022,
12 respectively. The results indicated that a 10 cm raise in the water table depth was able to slow down annual CO₂ emissions
13 from soil respiration by 0.87 Mg CO₂-C ha⁻¹. CH₄ fluxes changed from uptake to emissions with a raise in the water table
14 depth, and the maximum mean annual emission rate was 11 kg CH₄-C ha⁻¹. Nitrous oxide emissions ranged from 2 to 33 kg
15 N₂O-N ha⁻¹ year; they were high from bare soil in the beginning of the experiment but decreased towards the end of the
16 experiment. Short rotation cropping of willow reached net sequestration of carbon before harvest, but all treatments and years
17 showed net loss of carbon based on the net ecosystem carbon balance. Overall, the short rotation coppice of willow had the
18 most favourable carbon and greenhouse gas balance over the years (10 Mg CO₂ equivalent on the average over four years).
19 The total greenhouse gas balance of the forage and set-aside treatments did not go under 27 Mg CO₂ equivalent ha⁻¹ year⁻¹
20 highlighting the challenge in curbing peat decomposition in highly degraded cultivated peatlands.
21

22 Keywords: peatland, greenhouse gas, ground water table, paludiculture, land use
23

24 Graphical abstract



Photos: Jaana Nissi

25
26
27
28

29 **1. Introduction**

30 Cultivated peatlands are a major source of greenhouse gas (GHG) emissions globally (Strack et al., 2022). Conventional
31 cultivation requires lowering the water table depth (WTD) which makes all peat above the drainage depth prone to microbial
32 decomposition. Intensive management together with the high carbon and nitrogen content of peat makes agricultural peat
33 soils the highest CO₂ and N₂O emitters per unit area compared to any other land use types on peat soils (Maljanen et al.,
34 2010). Their GHG emissions currently diminish the net carbon sink of peat-rich countries significantly which can also be
35 turned to an advance: the climate change mitigation potential of drained peatlands is high (Humpenöder et al., 2020; Leifeld
36 and Menichetti, 2018) and cost per mitigated unit of CO₂ equivalent low (Lehtonen et al., 2022).

37 WTD is the major controller of GHG fluxes from peat soils (Evans et al., 2021; Wilson et al., 2016). A global meta-analysis
38 on water table manipulation studies showed that WTD explained most of the variation in GHG emissions but e.g. climate
39 zone had some influence as well (Huang et al., 2021). Rewetting has been found to diminish the release of CO₂ and N₂O from
40 decomposition but the switch from aerobic to anaerobic decomposition may change the ecosystem from a sink to source of
41 CH₄. However, the average increase in CH₄ emissions usually does not compromise the net GHG mitigation potential (Bianchi
42 et al., 2021; Guenther et al., 2020; Mander et al., 2023) but data is needed to understand the factors regulating CH₄ emissions
43 that can sometimes be high after rewetting (Nielsen et al., 2023).

44 Paludiculture, i.e. crop production in wet conditions on peat soils, is a GHG mitigation method that allows for slowing down
45 peat decomposition while still maintaining agricultural income from peatlands for the landowner (Tanneberger et al., 2022).
46 It is an opportunity for the agribusiness to improve the overall sustainability (Freeman et al., 2022; Liu et al., 2023) and it
47 produces clearly more societal benefits regarding ecosystem services than conventional management (Liu et al., 2023). As
48 regards to GHG mitigation, the raise in WTD reduces carbon losses from peat decomposition but export of carbon in the
49 harvest impairs the carbon balance of the system (Beetz et al., 2013). Emissions of N₂O are generally found to be low in
50 paludiculture (Bianchi et al., 2021) but they can remain high if fertilisers are applied (Bockermann et al., 2024). Emissions
51 of CH₄ are affected by the crop type, harvest management and N fertilisation (Boonman et al., 2023) but they can be efficiently
52 reduced by leaving an oxidised, non-waterlogged, layer on the peat surface to facilitate microbial oxidation of CH₄ (Kandel
53 et al., 2020). Solutions for paludiculture implementation are e.g. forage and willow that can be produced in wet conditions
54 because their roots improve the bearing capacity of the peat and thus ease machine work in wet conditions. Compared to
55 restoration to natural conditions, paludiculture leads to compromises, as both ecosystem services and economic productivity
56 are expected to be maintained, and it is not well known how these two aspects are best harmonised in practice. Set-aside is
57 often not a planned management option, but wet fields drift to non-productive use when the drainage system degrades, and
58 there are limited data on the GHG balance of such fields.

59 We established an experimental site with forage, willow and set-aside treatments in wet management on highly decomposed
60 cultivated peat soil in southern Finland in 2019-2023. As the target WTD of -20 cm below the surface was reached only
61 periodically, we cannot call the site a paludiculture site, but the results can be used to discuss the effects and practical issues
62 during the transition period to paludiculture. Our research questions were 1) What is the carbon and GHG balance of a
63 moderately rewetted drained peatland, 2) How much does harvesting reduce the potential to improve the carbon balance and
64 3) Do CH₄ emissions compromise the GHG mitigation in wet management?

67 **2. Materials and methods**

68 **2.1. The site and management**

69 The site was located in southern Finland (60.22 °N, 24.78 °E, 110 m a.s.l.) and it has been in cultivation at least since the 19th
70 century. The field has been in a crop rotation with cereals and grass during the latest decades. The climate is boreal humid

71 with long term (1991–2021) annual mean temperature of 5.2 °C and precipitation of 621 mm (Jokinen et al. 2021). The sum
 72 of annual global radiation is 3358 MJ m⁻² and total sunshine duration 1699 hours. Typically, the soil is frozen and has a snow
 73 cover from December to March-April. The field was a highly decomposed fen with peat depth ranging from 0.8 to over 2 m.
 74 Organic carbon content was 25% and pH 5.5 in the surface layer (0–20 cm) (Table 1). The original subsurface drainage
 75 system with tile drains was replaced by modern plastic pipes surrounded by gravel in the 1960s. The distance between the
 76 pipes was 18 m until 1979 when it was changed to 9 m. The drainage depth was 60–80 cm, and a control well was installed
 77 prior to the experiment to restrict water outflow and raise the ground water table. The adjustable tube inside the well was set
 78 to a position letting the water out when the water table reached 20 cm depth below the soil surface.

80 **Table 1:** Soil properties (\pm standard deviation) in the 0-20 cm layer in 2021

Variable	Value
Decomposition status (von Post)	8 (7-9)
Bulk density (g cm ⁻³)	0.39 \pm 0.05
Porosity (%)	0.80 \pm 0.02
Ash (%)	42 \pm 3.8
pH	5.4 \pm 0.09
C (g kg ⁻¹)	286 \pm 24.6
N (g kg ⁻¹)	15.2 \pm 1.24
Tot P (g kg ⁻¹)	0.97 \pm 0.08
Soluble P (g kg ⁻¹)	0.01 \pm 0.001
K (g kg ⁻¹)	0.17 \pm 0.03
Mn (g kg ⁻¹)	0.15 \pm 0.02
S (g kg ⁻¹)	2.01 \pm 0.13
Al (g kg ⁻¹)	1.41 \pm 0.12
Fe (g kg ⁻¹)	5.92 \pm 0.63

81
 82 The site was established in 2018 and it consists of twelve experimental plots (9 \times 6 m) in four blocks (see the graphical
 83 abstract). Four replicate plots with either grass mixture for forage (sown with *Poa trivialis* and *Festuca pratensis*, replanted
 84 in 2019 and 2021 with *Phleum pratense*, *Festuca pratensis*, *Lolium multiflorum* and *Poa pratensis*), bog bilberry (*Vaccinium*
 85 *uliginosum*; aka bog blueberry or bog whortleberry) or willow variety Klara (hybrid of *Salix schwerinii* Amgunkaja \times *Salix*
 86 *viminialis* Ivar) were randomly assigned within the four blocks. The grass was seeded and bilberry seedlings and willow
 87 saplings planted in June 2018 (Table S1). The bilberry did not grow roots, and those plots were left to develop to set-aside
 88 during the following years, thus we named this treatment as “set-aside”. The number of species in all twelve plots was
 89 determined once in the summer 2021.

91 2.2 Ancillary measurements

92 Biomass growth of willow was monitored by cutting three willow individuals from each plot for determining the above-
 93 ground biomass each June. The leaves, and stem + branches were separated and weighed to determine the fresh biomass. The
 94 woody biomass was cut in 10 cm pieces and dried at 65 °C for two weeks. The root biomass around one of the monitored
 95 plants per plot was determined by taking 50 \times 80 \times 20 cm peat samples from three layers: 0–20, 20–40 and 40–60 cm once
 96 per year. Visible large (>2 mm) and fine roots were manually separated from the peat, dried and weighed. For determining
 97 fine roots, the peat samples were mixed, and a 1 kg subsample was taken. Annual growth in stem, stool and coarse roots was
 98 calculated by subtracting the value from the previous year. Annual turnover rate of fine roots was assumed to be three times
 99 the biomass of fine roots as in Pacaldo et al. (2014). For example, biomass increment in 2019 was calculated with the
 100 following equation:

$$102 \text{ Annual Growth} = F_{19} + (S_{20} - S_{19}) + (St_{20} - St_{19}) + (Cr_{20} - Cr_{19}) + 3 * Fr_{19} \quad (1)$$

104 , where F19 is foliage in 2019, S19 and S20 are stems in 2019 and 2020, St19 and St20 are stools in 2019 and 2020, Cr19
105 and Cr20 are coarse roots in 2019 and 2020 and Fr19 is fine roots in 2019. Subsamples were taken for determining the C
106 content of the dried biomass in 2019 and 2020, and the mean values were used for the following years. The yield per hectare
107 was estimated to be the weight of 25,000 individuals, based on 80 cm × 50 cm spacing.

108 Soil temperature was measured first at the depth of 10 cm (but at the depth of 5 cm from May 2020 on to achieve better
109 response of CO₂ to air temperature) in each treatment with Elcolog sensors (Elcoplast Oy, Tampere, Finland). The sampling
110 rate was one hour in summer and 2.5 hours in winter. The air temperature, precipitation and radiation data were taken from
111 the Jokioinen weather station of Finnish Meteorological Institute (FMI 2024, CC BY 4.0) located about 10 km from the site.
112 Continuous photosynthetically active radiation (PAR) data was produced with global radiation data from FMI and corrected
113 using the ratio of 2.04 for global radiation and the PAR (Meek et al., 1984).

114 WTD was measured from monitoring pipes at the corners of the site at the time of the opaque chamber measurements until
115 2021 when monitoring pipes were installed also in the centre of each plot. During summers 2021 and 2022, there were also
116 HOBO Water Level data loggers (Onset, Bourne, United States) in each plot for continuous water level monitoring with a
117 sampling rate of one hour. In winter when the loggers were not used, WTD was measured manually from monitoring pipes
118 when the water was not frozen.

119 Leaf area index (LAI) was measured at the same time with the transparent chamber measurements with a portable LAI meter
120 (SunScan; Delta-T Devices Ltd, Cambridge, United Kingdom). LAI values > 3 were set to 3 as they were assumed to not
121 affect photosynthesis due to saturation of the reflectance (Aparicio et al., 2000). When harvesting the grass plots, the previous
122 measured LAI value was extrapolated to the moment just before harvesting, after which the LAI value was set to 1 as
123 measured. In 2022, we measured green canopy cover with the Canopeo app (Patrignani and Ochsner, 2015) instead of LAI.
124 Based on our experiences, and due to the operation and physical design of the LAI device, it did not provide as comprehensive
125 picture of the biomass inside the gas measurement collar as Canopeo. Vegetation index has been found to be faster to measure
126 and less dependent on the ambient light conditions than the light interception method (Shepherd et al. 2018). LAI was indexed
127 by dividing by maximum value 3 and green canopy cover by 100 (values from 0% to 100%) so that the generated vegetation
128 index range was 0–1. The vegetation index was set to 0 from the end of November until mid-April when the snow and frost
129 covered the ground or no green vegetation was present.

130 Soil samples for analysing the soil properties were taken first in October 2018 and another sampling was conducted in June
131 2021 with additional analysis. As there were no significant changes in the soil properties between these samplings, we present
132 only the results of the second soil sampling in Table 1. The samples were taken from the 0–20 cm layer using a soil corer with
133 a diameter of 3 cm. Approx. 20 subsamples were pooled to make composite sample that was air-dried and sieved (2 mm) for
134 the chemical analyses. Soil core samples for dry bulk density and porosity (diameter 5 cm) were taken from the surface layer
135 (0–17.5 cm) of each plot in Oct 2020 using the Kopec corer, and the samples were dried at 37 °C for a week. Soil acidity was
136 determined using the ISO 10390 method. Nutrient content was analysed as described in Vuorinen and Mäkitie (1955). Soil
137 carbon and nitrogen were determined using the dry combustion method (Leco TruMac CN, LECO corporation, MI).

138

139 **2.3. GHG measurements**

140 Dark respiration of the plants together with soil respiration (ecosystem respiration) and fluxes of N₂O and CH₄ were measured
141 using opaque chambers biweekly or once per month in the winter between 3/2019 – 3/2023. In each plot, a 60 cm × 60 cm
142 steel collar was installed at the depth of 10–15 cm. The location of the collars was one metre from the short edge of the plot
143 and three metres from the edges of the adjacent plots. An aluminium chamber (height 40 cm) mounted at the top of the collar
144 was sealed with water in the groove of the upper edge of the collar. In the winter, NaCl was added to the water to avoid ice
145 formation. The clear aluminium surface reflected effectively light and kept the temperature change moderate inside the
146 chamber. The measurements were done during the daytime between 10 am and 2 pm approximately every two weeks in

147 summertime, and monthly in the winter. The chambers were closed for 30 minutes, and four 20 ml gas samples were taken
148 with a 60-ml plastic syringe to pre-evacuated vials (Exetainer, Labco Limited, UK) in 10-minute intervals starting
149 immediately after closing. Prior to sampling, the syringe was pumped five times to mix the air in the chamber. The samples
150 were analysed with a gas chromatograph (Agilent 7890 Agilent Technologies, Inc., Wilmington, DE, USA) equipped with
151 flame ionizer and electron capture detectors, and a nickel catalyst for converting CO₂ to CH₄. The gas chromatograph had a
152 2 ml sample loop and a backflush system for separating water from the sample and flushing the precolumn between the runs.
153 The precolumn and analytical columns consisted of 1.8 and 3 m long steel columns, respectively, and were packed with
154 80/100 mesh Hayesep Q (Supelco Inc., Bellefonte, PA, USA). Nitrogen was used as the carrier gas and a standard gas mixture
155 of known concentration of CO₂, N₂O and CH₄ was used for a calibration curve with seven concentration points. An
156 autosampler (222 XL Liquid handler, Gilson Medical Electronics, France) fed the samples to the loop of the gas
157 chromatograph.

158 Net ecosystem exchange (NEE) including photosynthesis and respiration of the soil and plants was measured approximately
159 every two weeks during the growing season using a transparent chamber (60 × 60 × 60 cm) made of polycarbonate plexiglass
160 (1 mm, light transmission 95%). The chamber was equipped with a Vaisala GMP-343 probe for CO₂ measurement and a
161 temperature and humidity sensor (Vaisala Oy, Vantaa, Finland) and two fans for mixing the air during the measurement. PAR
162 was measured with LI-190 quantum PAR sensor (LI-COR, Lincoln, Nebraska, USA) inside the chamber. Four measurements
163 with different amount of entering light were taken from each plot on each measurement day in order to cover a large range of
164 light conditions and facilitate the gap filling by modelling. One or two layers of a white fabric shroud and one blackout curtain
165 were used to acquire measurement results in different light conditions (approximately 100%, 50%, 25%, 0% of ambient
166 radiation). The measurement with 0% radiation gave the estimate for ecosystem respiration (ER). The measurements were
167 done in the same collars as the opaque chamber measurements. Each measurement took one minute with a five second
168 sampling rate, or two minutes in early or late growing season when the change in flux was minor. The chamber was flushed
169 after each measurement to reconstitute ambient CO₂ and air humidity contents. After closing the chamber, a lag time of 10
170 seconds was applied to exclude the time when the flux was not yet stabilised. Clear sky conditions were preferred to avoid
171 problems related to changing cloud cover and to achieve the widest possible range of available light. The temperature change
172 inside the chamber was less than 1.5 degrees which was also used as a criterion for data filtering.

173 The change of CO₂ concentration during the chamber enclosure was assumed to be linear. The measurement results of CO₂
174 as parts per million (ppm) unit were converted to g m⁻² h⁻¹ by the ideal gas law using measured temperature inside the chamber.
175 If the flux was not yet stabilized at the beginning (first 4 datapoints) of the measurement, outliers were defined with Matlab
176 isoutlier command resulting removal of 210 of total 23066 datapoints in 1564 flux measurements.

177 If the snow cover was thicker than 20 cm, a concentration snow gradient method as in Maljanen et al. (2003) was used to
178 determine the GHG fluxes. A probe made of a steel pipe (Ø 3 mm), with a three-way valve and a plastic syringe, was used to
179 sample 15 ml of air just above the snow cover, in the bottom of the snow cover and at every 10 cm in between in three
180 replicate locations per plot. The gas was stored in the pre-evacuated vials and the concentrations were determined gas
181 chromatographically.

182 Measurements for bare soil respiration were made in unvegetated subplots in 7/2019–12/2022. For willow, the large 60 × 60
183 cm frames were used but for forage and set-aside we installed one sheet metal air ventilation pipe 27 cm in diameter and 30
184 cm in length to the depth of 5–10 cm next to the opaque chamber collars in the 8 plots of grass and set-aside. All green
185 vegetation within the chamber area was removed and root growth was limited by cutting around the chamber occasionally
186 with a knife. For the measurements, the cylinders were closed with a cover equipped with a CO₂ sensor (GMP-343; Vaisala
187 Oyj, Vantaa, Finland) and a small fan. One measurement lasted for one minute with a five second sampling rate.
188 Measurements were taken about once in a week or two, more frequently in summer than in winter. In winters 2021 – 2022

189 and 2022 – 2023 this method was not used due to too high snow depth but measurements with the snow gradient method were
190 utilized (Maljanen et al., 2003).

191

192 **2.4. Flux modelling**

193 Gross photosynthesis (GP) can be determined as the difference of NEE and ER. Instantaneous GP was estimated for each
194 measurement occasion by (equation 2),

195

$$196 \quad GP = NEE - ER \quad (2)$$

197

198 , where the full darkened transparent chamber measurement result (ER) is subtracted from the light-dependent flux (NEE)
199 measured during the same day. Thus, we follow the sign convention with positive ER and negative GP values.

200 The gaps in GP and ER data between the measurement occasions were predicted using hourly timeseries of the ancillary data.

201 Hourly time points for vegetation index, WTD and soil temperature and were acquired from the measured values by linear
202 interpolation. Gaps in soil temperature were filled with the modified soil temperature model (Zheng et al., 1993) using the air
203 temperature. Air temperature and PAR were assumed to be the same for all plots, whereas we used plot specific vegetation
204 index and the soil temperature from the certain treatment. Hourly ER and GP were modelled using nonlinear regression
205 (fitnlm function in MATLAB) for all 8 plots in forage and set-aside treatments. Empirical models were used for ER as in
206 Lohila et al. (2003) and for GP as in Kandel et al. (2013). Instead of the phytomass indices used in the above publications,
207 we used vegetation index formed according to the LAI and Canopeo measurements (index from 0 to 1) to describe the stage
208 of the crop growth.

209 We used the following equation first defined by (Long and Hällgren, 1993) for GP to estimate empirical coefficients (A_{max}
210 and k):

211

$$212 \quad GP = \frac{A_{Max} * PAR}{k + PAR} * VI * T_{Scale} \quad (3)$$

213

214 , where PAR is the measured photosynthetically active radiation ($\mu\text{mol m}^{-2} \text{s}^{-1}$), VI is the vegetation index, A_{max} is the
215 asymptotic maximum ($\text{g CO}_2 \text{ m}^{-2} \text{ h}^{-1}$), and k is a half-saturation value ($\mu\text{mol m}^{-2} \text{s}^{-1}$). T_{Scale} represents the temperature
216 sensitivity of photosynthesis and follows the equation presented by (Raich et al., 1991):

217

$$218 \quad T_{Scale} = \frac{(T - T_{min})(T - T_{max})}{(T - T_{min})(T - T_{max}) - (T - T_{opt})^2} \quad (4)$$

219

220 , where T is the measured temperature, photosynthetically active minimum temperature T_{min} is $-2 \text{ }^\circ\text{C}$, maximum T_{max} is $40 \text{ }^\circ\text{C}$
221 and the optimum is $20 \text{ }^\circ\text{C}$ as in (Kandel et al., 2013).

222 ER was estimated using data from the opaque and fully darkened transparent chambers. The empirical coefficients ($R0_s$, $R0_p$,
223 $E0_s$ and b) were estimated with a nonlinear regression model similarly as in the case of GP. Annual fluxes were computed as
224 sum of the hourly fluxes with a trapezoidal method (trapz function in Matlab 2019b). ER consists of autotrophic (R_{auto}), i.e.,
225 plant respiration and heterotrophic (R_{hetero}), i.e., soil respiration (LLOYD and TAYLOR, 1994) with extension of WTD as in
226 (Karki et al., 2014):

227

$$228 \quad ER = R_{hetero} + R_{auto} \quad (5)$$

$$229 \quad R_{hetero} = R0_s * \exp\left(E0_s \left(\frac{1}{56.02} - \frac{1}{T_{soil} + 46.02}\right)\right) + b * WTD \quad (6)$$

230 $R_{auto} = VI * R0_p * \exp(b_d(\frac{1}{10+273} - \frac{1}{T_{air}+273}))$ (7)

231

232 , where T_{soil} is the measured soil temperature, VI is the vegetation index, T_{air} is the measured air temperature, $R0_s$ is soil
233 respiration at the reference temperature 10 °C ($g\ CO_2\ m^{-2}\ h^{-1}$), $R0_p$ is plant respiration at the reference temperature at 10 °C
234 ($g\ CO_2\ m^{-2}\ h^{-1}$), b is the effect of WTD, $E0_s$ is ecosystem sensitivity and b_d is the temperature dependence of dark respiration
235 set to 5000 as in (Lohila et al., 2003). Bare soil respiration was estimated like ER but using only equation 6. The estimated
236 parameters $R0_s$, E_s and b and model R2 are shown in Table S3.

237

238

239

240 **2.5. Data processing and analysis**

241 For the transparent chamber measurements, the criterion $R^2 > 0.9$ for the fitted linear assumption of flux measurements would
242 exclude a large amount of data, especially with a small change in CO_2 , leading to a biased dataset. Therefore, we decided to
243 add the criterion $S_{xy} < 2.3\ g\ CO_2\ m^{-2}\ h^{-1}$ for dataset like in (Kutzbach et al., 2007) (S_{xy} is the standard deviation of the residuals
244 and $2.3\ g\ m^{-2}\ h^{-1}$ is the 95% percentile of measurements). This procedure resulted in the removal of 59 values out of total
245 1467 measurements. In the modelling phase, fitted values were examined, and outliers were removed to avoid distortion.
246 Outliers were defined as observations with an absolute value of standardised residuals greater than three. In 2019, 3 out of
247 260 GP values and 3 of 243 ER values were removed. In 2020, none of 200 GP values and 2 of 230 ER values were removed.
248 2 out of 365 GP values and 4 of 247 ER values were removed in 2021 and 12 out of 583 GP values and 2 of 323 ER values
249 were removed in 2022. The model's estimated parameters A_{max} , k of GP, $R0_s$, $R0_p$, E_s and b of ER and model correlations are
250 shown in Table S2. The measured versus model predicted values of GP and ER are shown by treatments and years in Fig. S1.
251 For bare soil respiration measurements in set-aside and forage, the same criteria were used as for transparent chamber ($R^2 >$
252 0.9 and $S_{xy} < 95\%$) leading to a removal of 12 values of total 601. In bare soil measurements in midsummer 2022, there
253 occurred 24 flux measurements (9 values in one plot, 0–5 in others) of total 147 values which were unexplained high (3–18
254 $g\ CO_2\ m^{-2}\ h^{-1}$). Values were of the same magnitude as values measured immediately after ploughing in (Honkanen et al.,
255 2023). We decided to remove these values as outliers to avoid model distortion. Soil respiration of willow was defined with
256 opaque chamber method and such outliers did not occur in these measurements. In modelling phase, outliers defined as
257 observations with an absolute value of standardised residuals greater than three, were removed resulting removal of 13
258 measurements of total 984 measurements (including all plots).

259 A linear regression model was fitted to calculate gas concentrations and the ideal gas law was used to solve the flux rate for
260 every enclosure of the opaque chambers. Nonlinear responses of CO_2 indicated a leaking chamber or other problem in the
261 measurement and thus, if the R^2 of CO_2 was less than 0.9, also the results of CH_4 and N_2O were discarded. In addition, sudden
262 variations in CH_4 fluxes due to ebullition were filtered by selecting only flux rates with the intercept between 1.5 and 2.4
263 ppm. These criteria resulted to 176, 117 and 118 discarded values out of 1044 in the case of CH_4 , CO_2 and N_2O , respectively.
264 All data cleaning and processing was done with Matlab (The Math Works, Inc., MATLAB, version 2019b).

265

266 **2.6. GHG balance**

267 The annual net ecosystem carbon balance was constructed as the sum of the hourly values of NEE and yield data for each
268 year in the case of forage and set-aside treatments. Modelling was used to fill the gaps between the measurement occasions
269 to create a continuous series of hourly values. For willow, annual estimates of carbon loss in soil respiration were available
270 from the chamber measurements from the unvegetated frames but as the willows were too high for the chambers their net
271 production had to be estimated based on biomass accumulation during four years (Pacaldo et al., 2014). The presented net
272 ecosystem carbon balance of willow is thus the sum of average annual CO_2 -C from soil respiration and average annual amount

273 of carbon bound in the biomass during the four first cultivation years. The cumulative annual fluxes of CH₄ and N₂O for each
 274 management practice were calculated by interpolating the emissions between consecutive sampling days. Global warming
 275 potentials 27 and 273 were used for CH₄ and N₂O, respectively, to convert the results to CO₂ equivalents for the total GHG
 276 balance (Forster et al. 2021).

277

278 2.7. Statistical analyses

279 Linear mixed models were used to find variables explaining variation in the gas fluxes. Crop, year, WTD and all their
 280 interactions were denoted as fixed effects. Block and block × year were assumed to be independent and normally distributed
 281 random effects. The most suitable covariance structure was chosen using Akaike's Information Criterion (AIC). The models
 282 were fitted using the residual maximum likelihood (REML) method and degrees of freedom were estimated using the
 283 Kenward-Roger method. The residuals were plotted against the fitted values and the normality of the residuals were checked
 284 using boxplots. The data was log--transformed when needed to normalise the distributions. The method of Tukey-Kramer
 285 was used for all pairwise comparisons of means with a significance level of 0.05. After the first model run with all relevant
 286 variables the non-significant variables were removed one by one to find the most relevant effects. All statistical analyses were
 287 performed using the SAS Enterprise Guide v7.1 (SAS Institute Inc., Cary, NC, USA).

288

289 3. Results

290 3.1 Climate and site variables

291 Annual mean temperature was 6.9, 6.0, 5.8 and 5.8 °C and annual precipitation 750, 600, 660, and 546 mm in 2019 – 2022,
 292 respectively. Number of days with a snow-cover on the soil within each modelling year (April to March) was 13, 81, 108 and
 293 118, respectively. The annual mean temperature during the study years was higher than the long-term average of 5.2°C in
 294 1991–2020 (Jokinen et al., 2021). Two study years exhibited lower and two higher annual precipitation as compared to the
 295 long-term mean of 621 mm. The WTD showed an increasing trend in time and high within-year variation (Fig. 1). The average
 296 WTD was -54, -41, -39 and -27 cm in 2019–2022, respectively. WTD varied from -89 to -4, -77 to 2, -120 to 1.4 and -100 to
 297 1.8 cm in 2019 – 2022, respectively.

298 The forage yields were 6.3±0.9, 8.9±0.7, 11±0.8 and 9.4±0.9 Mg DM ha⁻¹ in 2019-2022, respectively. There were two harvests
 299 in 2020 and three in the other years. The plots were dominated by *Phleum pratense* and *Festuca pratensis* in 2021. The dry
 300 mass yields of willow were 30±14 and 73±28 Mg DM ha⁻¹ in the harvests of February 2021 and 2023. Most of the C
 301 accumulation occurred in the stem (59%), followed by stool (25%) and roots (9%) and foliage (7%) (Table 2). Vegetation of
 302 the set-aside plots in 2021 was dominated by wild plants belonging to Families *Asteraceae*, *Cichoriaceae* and
 303 *Caryophyllaceae*. Bog bilberry covered one percentage or less on each of the four replicate plots. The set-aside vegetation
 304 had the highest species diversity, 19 vascular plants compared to 12 at willow plots and 9 at forage plots, the two latter
 305 including crop plants.

306

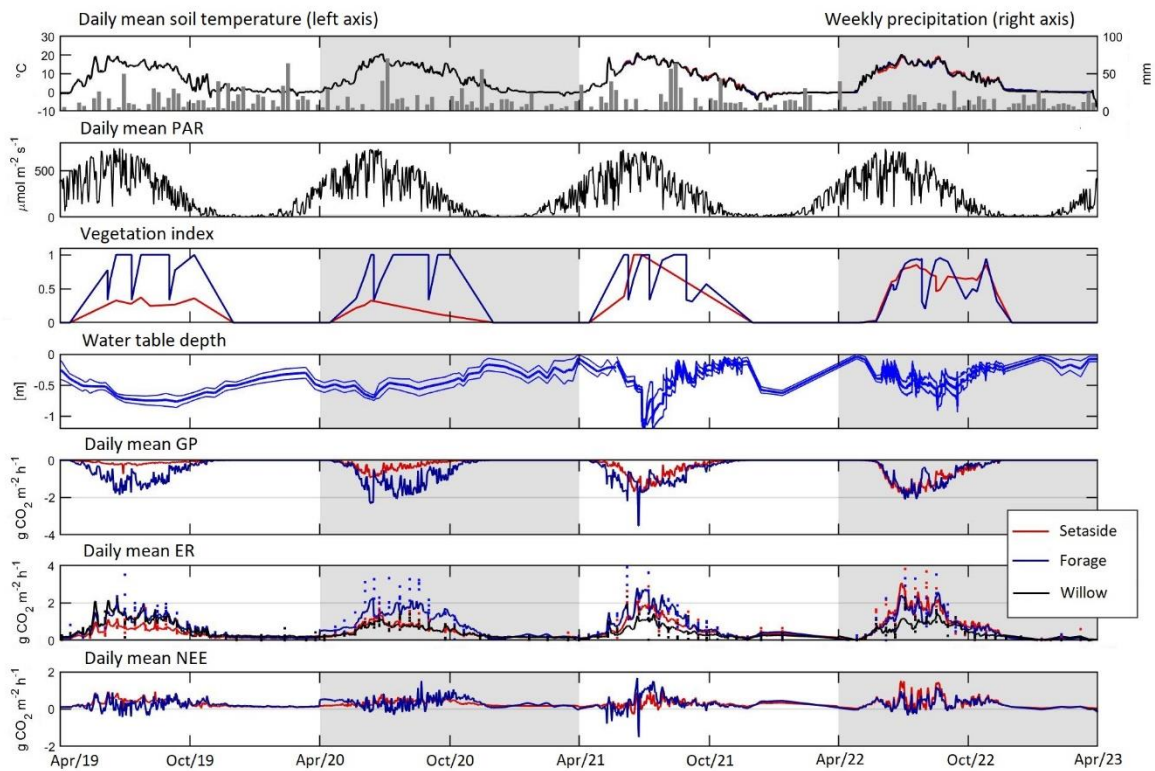
307 **Table 2:** Four-year cumulative carbon balance of willow (±standard deviation). Negative sign indicates sequestered carbon
 308 and positive sign released carbon to the atmosphere.

Component	Mg C ha ⁻¹ 4 yrs ⁻¹	% of total
Stem (harvested)	-50.7±14.3	59
Foliage	-6.2±0.8	7
Aboveground stool	-12.6±3.2	15
Underground stool	-8.5±3.8	10
Coarse roots	-3.9±1.5	4
Fine roots	-4.6±0.6	5
Total sequestered carbon	-86.5±19.5	

Soil respiration	43.5±2.7
Net ecosystem exchange	-43.1±21.1
Net ecosystem carbon balance	7.6±7.7

309

310



311

312 **Figure 1:** Daily mean of soil temperature and precipitation, photosynthetically active radiation (PAR),
 313 vegetation index,
 314 water table depth (site mean±std), gross photosynthesis, measured (dots) and model predicted (line) ecosystem respiration
 315 (soil respiration for willow) and net ecosystem exchange. Annual modelling periods (Apr - Mar) are marked with light grey
 or white background.

316

317

318 3.2. Carbon balance

319 Model predicted maximum hourly GP was -0.7, -3.2, -4.3 and -4.8 g CO₂ m⁻² h⁻¹ in the set-aside in 2019 – 2020, and -3.9, -
 320 5.9, -4.3 and -4.8 g CO₂ m⁻² h⁻¹ in the forage plots in 2019–2022, respectively (Fig. S1). Maximum measured GP value was
 321 -1.1, -2.4, -3.4 and -4.5 g CO₂ m⁻² h⁻¹ for set-aside and -3.4, -6.2, -4.8 and -4.2 g CO₂ m⁻² h⁻¹ for forage in 2019–2020,
 322 respectively. Annual values of GP varied from -9.3 to -12 Mg CO₂-C ha⁻¹ yr⁻¹ in the forage and from -1.5 to -10 Mg CO₂-C
 323 ha⁻¹ yr⁻¹ in the set-aside treatment (Table 3). The variables initially included in the analysis were annual mean WTD, crop
 324 type and year as main effects and all their interactions. Finally, only crop, year and their interaction were left in the model
 325 (Table S4). Inclusion of WTD did not result in a meaningful estimate as both the productivity of especially the set-aside
 326 established in 2019 and the WTD increased with years, and the observed change in GP did not in reality increase with WTD
 327 but with time. Forage and set-aside treatments differed significantly (p<0.001), there was an increasing trend in
 328 productivity from 2019–2022 (p=0.0009) and the differences between the crop types were highest in 2019–2021 (p<0.001).

329

331 **Table 3:** The estimated annual sums (\pm standard deviation) of gross photosynthesis (GP), ecosystem respiration (ER), net
 332 ecosystem exchange (NEE), carbon exported in the harvested yield, net ecosystem carbon balance (NECB), N₂O and CH₄
 333 effluxes and the total emissions (global warming potential of one hundred years; GWP-100) with either NEE or NECB
 334 representing CO₂ emissions in the forage and set-aside plots, and selected data for willow. Significant differences ($p < 0.05$)
 335 between treatments within a year are denoted with different letters ($n=4$).

Year	Variable and unit	Forage	Set-aside	Willow ^a
2019	GP Mg CO ₂ -C ha ⁻¹	-9.31 \pm 0.75a	-1.48 \pm 0.32b	
	ER Mg CO ₂ -C ha ⁻¹	14.4 \pm 2.17a	8.25 \pm 2.40b	
	NEE Mg CO ₂ -C ha ⁻¹	5.08 \pm 1.80	6.77 \pm 2.41	
	C in yield Mg C ha ⁻¹	3.17 \pm 0.49	0	
	NECB Mg C ha ⁻¹	8.25 \pm 2.13	6.77 \pm 2.41	
	Soil respiration Mg CO ₂ -C ha ⁻¹	12.8 \pm 4.99	11.4 \pm 1.82	14.8 \pm 0.76
	N ₂ O-N kg ha ⁻¹	11.9 \pm 7.60a	32.6 \pm 12.1b	17.4 \pm 10.3
	CH ₄ -C kg ha ⁻¹	-0.28 \pm 0.75	-1.00 \pm 0.73	-1.64 \pm 0.26
	GWP ₁₀₀ Mg CO ₂ eq ha ⁻¹ (NEE) ^b	23.7 \pm 5.67	38.8 \pm 19.8	
	GWP ₁₀₀ Mg CO ₂ eq ha ⁻¹ (NECB) ^c	35.3 \pm 6.86	38.8 \pm 19.8	
2020	GP Mg CO ₂ -C ha ⁻¹	-11.7 \pm 1.17a	-3.57 \pm 0.46b	
	ER Mg CO ₂ -C ha ⁻¹	19.3 \pm 1.85a	10.6 \pm 1.49b	
	NEE Mg CO ₂ -C ha ⁻¹	7.64 \pm 1.75	7.05 \pm 1.12	
	C in yield Mg C ha ⁻¹	3.35 \pm 1.28	0	
	NECB Mg C ha ⁻¹	11.0 \pm 2.02	7.05 \pm 1.12	
	Soil respiration Mg CO ₂ -C ha ⁻¹	9.09 \pm 4.86	10.6 \pm 0.97	10.0 \pm 0.79
	N ₂ O-N kg ha ⁻¹	6.26 \pm 3.39	6.59 \pm 2.97	4.61 \pm 2.99
	CH ₄ -C kg ha ⁻¹	-0.36 \pm 0.40	-1.01 \pm 0.56	-1.13 \pm 0.33
	GWP ₁₀₀ Mg CO ₂ eq ha ⁻¹ (NEE)	30.4 \pm 7.64	28.7 \pm 3.73	
	GWP ₁₀₀ Mg CO ₂ eq ha ⁻¹ (NEBC)	42.6 \pm 8.69	28.7 \pm 3.73	
2021	GP Mg CO ₂ -C ha ⁻¹	-9.46 \pm 1.20a	-6.34 \pm 0.68b	
	ER Mg CO ₂ -C ha ⁻¹	17.4 \pm 1.40a	13.5 \pm 1.82b	
	NEE Mg CO ₂ -C ha ⁻¹	7.95 \pm 2.16	7.12 \pm 2.16	
	C in yield Mg C ha ⁻¹	5.54 \pm 0.46	0	
	NECB Mg C ha ⁻¹	13.5 \pm 1.88a	7.12 \pm 2.16b	
	Soil respiration Mg CO ₂ -C ha ⁻¹	7.82 \pm 2.30	11.5 \pm 2.44	8.99 \pm 2.70
	N ₂ O-N kg ha ⁻¹	6.49 \pm 3.88a	2.18 \pm 0.24b	5.75 \pm 6.25
	CH ₄ -C kg ha ⁻¹	7.92 \pm 12.7	0.58 \pm 1.87	3.89 \pm 6.12
	GWP ₁₀₀ Mg CO ₂ eq ha ⁻¹ (NEE)	32.2 \pm 8.16	27.1 \pm 8.03	
	GWP ₁₀₀ Mg CO ₂ eq ha ⁻¹ (NEBC)	52.2 \pm 6.93	27.1 \pm 8.03	
2022	GP Mg CO ₂ -C ha ⁻¹	-9.34 \pm 2.13	-9.65 \pm 2.08	
	ER Mg CO ₂ -C ha ⁻¹	14.4 \pm 3.29	16.5 \pm 3.21	
	NEE Mg CO ₂ -C ha ⁻¹	5.10 \pm 1.15	6.82 \pm 1.15	
	C in yield Mg C ha ⁻¹	4.72 \pm 0.50	0	
	NECB Mg C ha ⁻¹	5.46 \pm 6.37	6.82 \pm 1.15	
	Soil respiration Mg CO ₂ -C ha ⁻¹	8.40 \pm 1.48	15.0 \pm 5.32	9.70 \pm 2.3
	N ₂ O-N kg ha ⁻¹	9.54 \pm 4.49a	3.07 \pm 0.86b	1.69 \pm 1.10b
	CH ₄ -C kg ha ⁻¹	7.74 \pm 0.59	11.3 \pm 7.72	10.9 \pm 12.9
	GWP ₁₀₀ Mg CO ₂ eq ha ⁻¹ (NEE)	22.9 \pm 3.34	26.6 \pm 4.61	
	GWP ₁₀₀ Mg CO ₂ eq ha ⁻¹ (NEBC)	43.3 \pm 3.18	26.6 \pm 4.61	

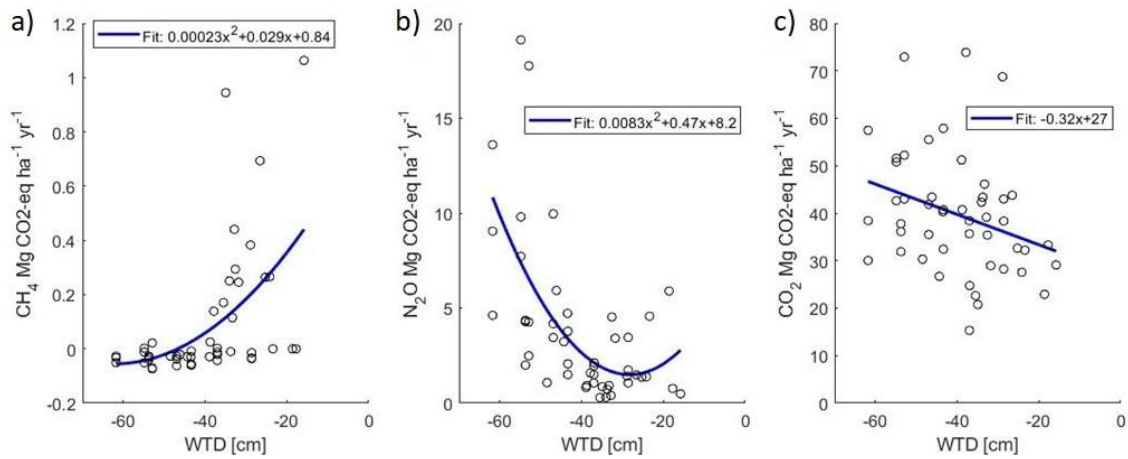
336 ^aAll components of the carbon balance are not available for willow, see chapter 2.6, ^bWith NEE representing CO₂, ^cWith
 337 NEBC representing CO₂

339 Modelled maximum hourly ER was 2.4, 2.3, 3.0 and 4.7 g CO₂ m⁻² h⁻¹ in the set-aside and 3.5, 3.4, 4.8 and 4.5 g CO₂-C m⁻²
340 h⁻¹ in the forage plots (Fig. S1). Measured maximum ER with the opaque chamber method was 1.7, 2.0, 2.9 and 4.6 g CO₂-C
341 m⁻² h⁻¹ for the set-aside and 3.5, 4.2, 4.0 and 4.8 g CO₂-C m⁻² h⁻¹ for forage. Annual ER varied from 14 to 19 Mg CO₂-C ha⁻¹
342 yr⁻¹ in the forage and from 8 to 17 Mg CO₂-C ha⁻¹ yr⁻¹ in set-aside treatment (Table 3). Variables initially included in the
343 analysis were annual mean WTD, crop type and year as main effects as well as their interactions. WTD did not well explain
344 the variation in the annual ER estimate, likely for the same reason as for GP as plant respiration is related to the biomass of
345 the vegetation, which increased during the experimental years. The best model was based on the crop type and year as main
346 effects, and their interactions (Table S4). In this model, crop type explained ER well, ER increased in time, and ER increased
347 between years more in forage than set-aside.

348 Hourly model-predicted NEE varied from -2.9 to 3.7 g CO₂ m⁻² h⁻¹ in the set-aside and from -4.6 to 3.7 g CO₂ m⁻² h⁻¹ in the
349 forage treatment (results not shown). There were 29, 28, 16 and 47 days annually with negative daily NEE in the forage plots
350 during the study years, respectively, and fewer such days (1, 0, 9 and 6) in the set-aside plots in 2019–2022 (Fig. 1). The
351 cumulative annual balance ranged from 5.1 to 8.0 Mg CO₂-C ha⁻¹ yr⁻¹ in the forage and from 6.8 to 7.1 Mg CO₂-C ha⁻¹ yr⁻¹ in
352 the set-aside treatment (Table 3) and the treatments did not differ statistically. The net ecosystem carbon balance (NECB)
353 that accounts the amount of carbon exported in the harvested yield varied from 5.5 to 13.5 Mg CO₂-C ha⁻¹ yr⁻¹ in the forage
354 treatment and were equal to NEE in the set-aside treatment (Table 3). The NECB values differed statistically between the
355 forage and set-aside treatments across all years (p>0.001) and inclusion of additional effects in the analysis did not improve
356 the model (Table S4).

357 Annual sum of respiration varied from 8 to 15 Mg CO₂-C ha⁻¹ yr⁻¹ in the different treatments and years (Table 3). The
358 proportion of soil respiration of the total ecosystem respiration varied from 45 to 90% in the forage plots and from 85 to 100%
359 in the set-aside plots in 2019–2022. In the set-aside plots, estimated annual bare soil respiration exceeded the estimated ER
360 in all plots in 2019, two plots in 2020 and one plots in 2021 and 2022 and those values were not used in the above calculation,
361 and thus it is assumed that total respiration constituted only of soil respiration in 2019. Annual cumulative soil respiration
362 was explained by WTD (Fig. 2; p=0.053) and crop type (p=0.033) so that forage and set-aside treatments were significantly
363 different in the whole dataset and respiration increased in the order forage<willow<set-aside (Fig. S4; Table S4). Plots of the
364 bare soil respiration in relation to WTD and temperature show that there is a clear trend of decreasing respiration with raising
365 WTD (Fig. S2). Three individual curves indicate a contrasting trend, but these three estimations are based on a small number
366 of measurement results. Based on all annual estimates of soil respiration, a 0.1 m raise in WTD reduces respiration by 0.87
367 Mg CO₂-C ha⁻¹ yr⁻¹.

368 The cumulative total amount of C in the above and below ground willow biomass was 86.5 Mg C ha⁻¹ during the four study
369 years (Table 2). About 40% of the carbon in the biomass was left at the site after harvest, and soil respiration amounted to
370 43.5 Mg ha⁻¹, leading to a strongly negative cumulative NEE of -43 Mg ha⁻¹. Carbon export in the harvest changed the net
371 balance to net loss of 7.6 Mg, corresponding to an average annual CO₂ rate of 7 Mg of CO₂.



373

374

375

Fig. 2. Plot-wise mean annual fluxes of CH₄ (a), N₂O (b) and soil respiration (c) (CO₂ eq.) as related to the mean annual WTD.

376

377

378

379 3.3. CH₄ fluxes

380

381

382

383

384

385

386

387

388

Hourly fluxes of CH₄ varied between -50 and 30 μg CH₄-C m⁻² h⁻¹ during the first half of the experimental period (Fig. 3). In conjunction with the raise in the WTD the values the hourly fluxes increased and varied between -40 and 900 μg m⁻² h⁻¹ during the latter half of the period. The annual flux of CH₄ varied from -1.6 to 11 kg CH₄-C ha⁻¹ yr⁻¹ with an increasing trend towards the end of the measurement period (Table 3; Fig. S3). When the mean annual WTD was below 40 cm the soil was mainly consuming CH₄, but the consumption tended to change to emissions as the WTD raised (Fig. 2). Variation in the annual cumulative fluxes of each plot was explained by the WTD (p=0.015) but not by crop (Table S4). The increasing trend between years 2019–2022 was also shown in the mixed model analysis as year had a significant effect (p=0.0003) and the effect of WTD decreased with time (years).

389

390 3.4. N₂O fluxes

391

392

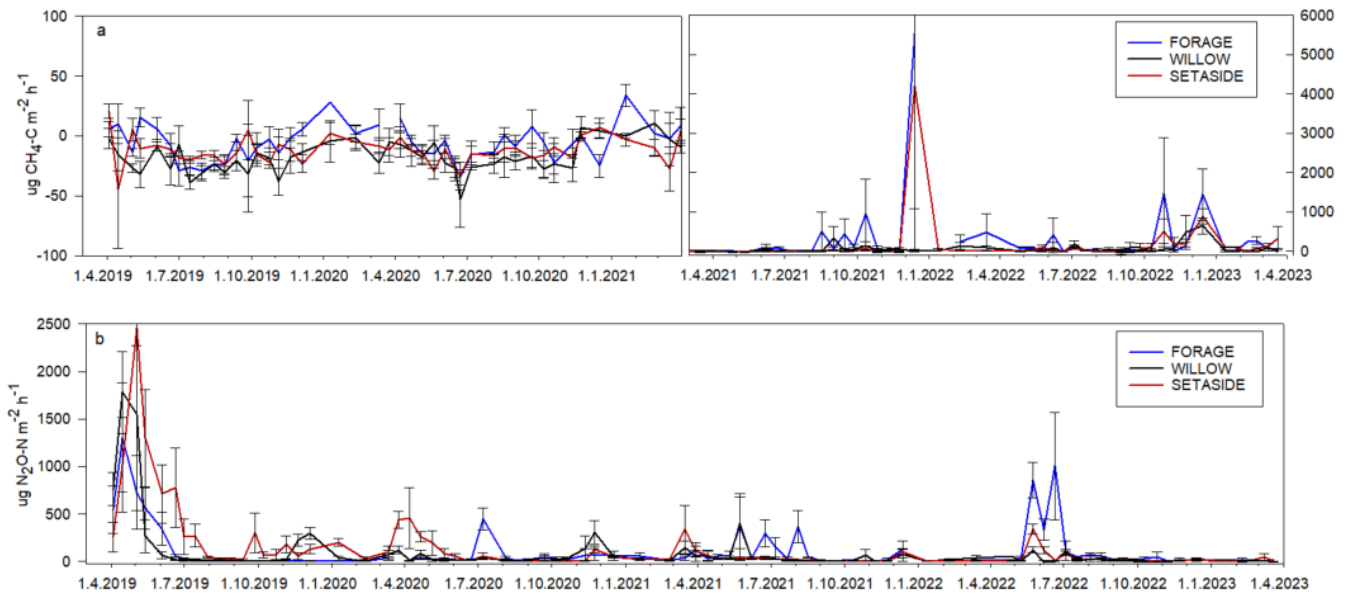
393

394

395

396

Hourly fluxes of N₂O varied between -3 and 2500 μg N₂O-N m⁻² h⁻¹ during the four years with the highest emissions during the first four months (Fig. 3). Annual fluxes of N₂O varied from 1.7 to 33 kg N₂O-N ha⁻¹ yr⁻¹ (Table 3). The emissions declined in time (Fig. S3) especially in the case of set-aside and willow whereas those of forage did not show such a trend (Table 3). WTD explained variation in N₂O fluxes well (p=0.015) (Fig. 2; Table S4). There were some interactions of year and crop, but the crop type did not affect N₂O emissions systematically between years. Annual N₂O fluxes of the forage and willow treatments differed in the whole timeseries (p=0.026).



397

398

399

Fig. 3. Fluxes of CH₄ (a) and N₂O (b) in 2019-2023. The error bars denote standard error. Note the different scale in the y-axis of (a) for the latter half of the period.

400

401

402

3.5. Global warming potential

403

404

405

406

407

408

409

The total emissions expressed as CO₂ equivalents ranged from 23 to 39 Mg ha⁻¹ yr⁻¹ with NEE as the CO₂ component and from 27 to 52 Mg with the C export in harvest taken into account in the forage and set-aside treatments (Table 3). For willow, the annual NECB cannot be calculated but based on the four-year estimate on carbon binding in the biomass and carbon exported in the harvest divided to a single year, together with the average annual soil respiration and N₂O and CH₄ fluxes, the average annual climate impact of willow cultivation was 10.2 Mg ha⁻¹ yr⁻¹.

410

411

412

413

414

415

416

417

418

419

420

421

422

423

424

425

426

4. Discussion

NEE values of 5–8 Mg C ha⁻¹ per year in the forage plots were of the same magnitude as values reported for grass cultivation in northern Europe (Maljanen et al., 2010). They were, however, 6–10 times higher than NEE reported for year 2002 in a nearby field (Lohila et al., 2004), highlighting the spatial and temporal variation in soil emissions. During the first two years of the experiment, the CH₄ fluxes of the forage plots were negative indicating net consumption of CH₄ by the soil microorganism. The CH₄ oxidation rates were generally higher than average values reported from Nordic cultivated peat soils which have shown net positive values for grass fields (Maljanen et al., 2007, 2010). There was a change from negative fluxes of CH₄ to relatively high emissions after the annual mean water table rose above -40 cm during the two latter years of the experiment. However, compared to rewetted agricultural sites in the temperate zone, the values of ca. 8 kg CH₄-C per hectare were clearly lower than the average of 180 kg CH₄-C ha⁻¹ yr⁻¹ found in temperate paludiculture-like grassland ecosystems (Bianchi et al., 2021). The N₂O emissions ranging from 6 to 12 kg N per hectare annually were typical for northern European grass fields on organic soils as they were within the 95% confidence interval of the reported values from temperate and boreal regions (Hiraishi et al., 2014). After the high emission peak in the beginning of the experiment there were only short-term peaks after fertilisation. One of them was especially high and long-lasting and likely induced by heavy rainfall after a long dry period coinciding with fertilisation in May-June 2022. It is typical that high peaks after fertilisation occur when fertilisation is followed by rainfall (Dobbie et al., 1999), and fertiliser-induced peaks may be totally absent if there is no coinciding rainfall (Beetz et al., 2013). The set-aside plots with slowly evolving vegetation had clearly lower GP than the forage plots during the three first years. However, also the ER was lower in the set-aside, and the resulting NEE was of the

427 same magnitude in both treatments. Because there was no biomass export from the set-aside the NECB was lower than in the
428 forage treatment in most years. The modelled NEE values were about double compared to long-term abandoned croplands in
429 the Nordic countries (Maljanen et al., 2010) but in our study the plots did not represent similar ecosystems as they were
430 “abandoned” only for a short period. N₂O fluxes of the set-aside plots were extremely high in 2019 compared to results of
431 previous studies on cultivated peat soils in Nordic countries (Maljanen et al., 2010). As the “set-aside” was fertilised and
432 unsuccessfully planted with bog bilberry, the high emissions were likely due to abundant free mineral nitrogen in the absence
433 of plant nutrient uptake. As the berry plants did not thrive, the soil was bare for a long period and the N₂O emissions remained
434 higher than in the other treatments throughout the summer. Such conditions were prevailing also in a similar bare fallow
435 treatment at a nearby site in 2000-2002, yielding average N₂O emissions of 25 kg N ha⁻¹ yr⁻¹ (Regina et al., 2004). During the
436 second year, the emissions lowered but as the plots were fertilised also in 2020, they still exhibited as high emissions as the
437 forage plots. During the last two years the N₂O emissions were at a notably low level which likely resulted from ceasing of
438 fertilisation and a slightly higher WTD leading to less peat being exposed to aerobic conditions. Raising the WTD has been
439 found to diminish N₂O emissions in several studies (van Beek et al., 2010; Leppelt et al., 2014).

440 Willow grew well at this site and the mean annual yields were in the higher end of the range 4-16 Mg ha⁻¹ estimated for
441 northern climate conditions (Viherä-Aarnio et al., 2022). Carbon lost in soil respiration was lower than the amount sequestered
442 in the willow biomass in all years except in 2019, leading to highly negative NEE during the whole rotation. However, the
443 amount of carbon exported in harvest exceeded the NEE and the yielding NECB indicated net loss of carbon to the
444 atmosphere. Although the average annual NECB calculated from the four-year carbon balance (1.9 Mg C ha⁻¹ yr⁻¹) was low
445 compared to the forage or set-aside treatments, it still indicated a climate-warming end result in short-rotation cropping of
446 willow on peat soil. It is possible to achieve a net positive NEBC in willow cultivation on mineral soils (Harris et al., 2017;
447 Morrison et al., 2019) but in peatlands the high rate of soil respiration inevitably reduces this potential (Kasimir et al., 2018).
448 The target WTD was not reached for most of the time likely because there was unexcepted lateral water outflow from the
449 site. Our strategy of raising the WTD at a limited area within a field parcel was thus not successful. The larger the area where
450 the water outflow is restricted, the better the result likely is, and catchment level water management planning is often
451 recommended for the best results (Mitsch and Wilson, 1996; Pasquet et al., 2015).

452 The annual emissions can be compared to a well-drained cereal site (oats; mean WTD 68 cm) on the same field (Honkanen
453 et al., 2023), as the distance between these two experiments was just about 20 m. In 2020, when similar measurements were
454 conducted in both experiments, the total GHG balance (GWP100 with harvest) was 29 Mg in the set-aside and 43 Mg in the
455 forage treatment while it was 39 Mg CO₂-eq. in the conventionally managed cereal plots. As the comparable number for
456 willow was 10 Mg in the willow treatment, it can be argued that the set-aside and willow cultivation with a moderate raise of
457 WTD were better management options than cultivation of annual crops with a typical drainage depth. It was also clear that
458 willow had the best GHG balance of these three management options, which is in agreement with findings of grassland and
459 willow cropping in southern England (Harris et al., 2017). However, the total emissions were still relatively high suggesting
460 that this kind of moderately wet management is not an efficient climate mitigation measure. This was also shown by the
461 modelling results of (Kasimir et al., 2018) concluding that fully rewetted peatland had the most favourable carbon balance
462 and less emissions from soil in a comparison of four different peatland management scenarios. However, management
463 decisions, like cutting height also play a role in determining the final carbon balance in short-rotation cropping (Berhongaray
464 et al., 2017).

465 Set-aside is a relevant management option to study because many cultivated peat fields end up as uncultivated plots when
466 their drainage system degrades, and the landowner finds them too wet for cultivation. The annual total emissions were lower
467 in the set-aside plots compared to the forage in 2020 and 2021, and also in 2022 if the carbon exported in harvest is taken into
468 account. However, they were not especially low as compared to cultivated peat soils in general. Thus, leaving cultivated peat
469 soils uncultivated without active rewetting is not desirable form of land management as these sites drift out from food

470 production, but the GHG emissions can remain high. A recent Swedish study also found that setting aside did not reduce
471 GHG emissions from a drained peat soil (Keck et al., 2024)

472 Our set-aside plots were actually intended to be vegetated by bog bilberry, a native mire plant that could become a novel
473 antioxidant-rich ingredient for food (Lätti et al., 2010) or pharmaceutical (Esposito et al., 2019) industries. However, we soon
474 noticed that the seedlings did not grow roots indicating that formerly agriculturally cultivated peat was not a suitable substrate
475 for this plant. As the nutrient content of the topsoil did not show large deviations from the reported ranges supporting the
476 growth of bog bilberry (Jacquemart, 1996), it is likely that the pH of 5.4 at our site was too high. Bog bilberry is usually found
477 in soils with pH below 5. However, in recent trials it has been successfully grown on Chinese farmlands with pH 5–6 but low
478 pH improved the growth also there (Duan et al., 2022).

479 There are usually high uncertainties in the GHG measurements, and this is especially true regarding the combination of
480 methods chosen for the willow treatment. The carbon balance of willow was determined using a combination of the pool-
481 based and flux-based methods, which can differ by several magnitudes (Berhongaray et al., 2017). The most reliable method
482 for measuring the carbon balance of willow stands is likely the eddy covariance method, which is not feasible in experiments
483 with small plots. Part of the uncertainty also arises from the simplicity of the models. For example, soil respiration was
484 modelled only based on soil temperature and WTD, although it can be affected also e.g. by changes in microbial community
485 composition or activity (Yang et al. 2022) and soil moisture which does not always well follow changes in WTD (Smith et
486 al. 2018). Estimating vegetation cover using measured LAI is also problematic, as it reflects weakly the amount of active
487 chlorophyll (Delegido et al., 2015; Gregersen et al., 2013). It is especially difficult to assess active vegetation at the beginning
488 and end of the growing season. However, the influence on the annual balance is minor due to low temperature and radiation
489 at that time. With the Canopeo application, the models were significantly better as it was possible to determine the green leaf
490 area better than with the previously used LAI measurement with the SunScan instrument. The measurement results of PAR
491 values feature uncertainties due to abrupt changes in cloudiness or fogging and dirt on the plexiglass. Due to technical
492 problems, FMI data and another PAR sensor was used to fill the gaps in the PAR measurements especially in 2021. The
493 plexiglass surfaces were kept as clean as possible, fogging was kept low by using a short measurement time, and clear sky
494 conditions were preferred which should reduce the uncertainty occurred in measurements. Model predicted soil temperature
495 in gap filling may cause some error, but the filled gaps were not long, and the error was mostly diurnal with low significance
496 for the annual balances. Regarding biweekly N₂O and CH₄ measurements, there is a high risk of missing short-term peaks,
497 for example due to freeze-thaw cycles (Lammirato et al., 2021). Also, if the measurements hit peaks, the emissions may be
498 overestimated due to interpolation of the gaps in the data particularly during times with infrequent measurements.

499

500 **5 Conclusions**

501 This study gave valuable insights to the practical implementation and climate mitigation potential of three management
502 options relevant for cultivated peatlands with raised WTD: forage, willow and set-aside. The results indicate that wet
503 management of cultivated peat soils considerably reduces the soil respiration and N₂O emissions. Significant counteracting
504 effect of increased CH₄ emissions are avoided as long as the WTD does not rise close to the soil surface. However, compared
505 to full rewetting, partial rewetting remains a compromise solution to climate warming as it is likely that the peat layer will
506 eventually be lost. It is important to develop incentives to inundate large, connected peatland areas to ensure water availability
507 and maintenance of high enough water table for efficient control of peat decomposition.

508

509 **Authorship contributions.** KL and HK designed the experiment. JH, HH, SS and TL developed the methodology. HK and
510 TL planned, supervised and partly conducted the field work. KL, HH and HK analysed and visualised the data. KL and HH
511 wrote the original manuscript. All authors were involved in revising the text.

512

513 **Data availability.** The data will be available in Zenodo two years after publication.

514

515 **Competing interests.** The contact author has declared that none of the authors has any competing interests.

516

517 **Acknowledgements.** The authors are grateful to the technical staff of Natural Resources Institute Finland for skilled work in
518 the field and laboratory.

519

520 **Financial support.** This study was part of the project SOMPA (Novel soil management practices – key for sustainable
521 bioeconomy and climate change mitigation), funded by the Strategic Research Council at the Research Council of Finland,
522 grant No 312912 and INSURE (Indicators for successful carbon sequestration and greenhouse gas mitigation by rewetting
523 cultivated peat soils) subproject of the EJP Soil project that has received funding from the European Union’s Horizon 2020
524 research and innovation programme under grant agreement No 862695.

525

526

527

528

529 **References**

530 Aparicio, N., Villegas, D., Casadesus, J., Araus, J. L., and Royo, C.: Spectral Vegetation Indices as Nondestructive Tools
531 for Determining Durum Wheat Yield, *Agron. J.*, 92, 83–91, <https://doi.org/10.2134/agronj2000.92183x>, 2000.

532 van Beek, C. L., Pleijter, M., Jacobs, C. M. J., Velthof, G. L., van Groenigen, J. W., and Kuikman, P. J.: Emissions of N₂O
533 from fertilized and grazed grassland on organic soil in relation to groundwater level, *Nutr. Cycl. Agroecosystems*, 86, 331–
534 340, <https://doi.org/10.1007/s10705-009-9295-2>, 2010.

535 Beetz, S., Liebersbach, H., Glatzel, S., Jurasinski, G., Buczko, U., and Hoepfer, H.: Effects of land use intensity on the full
536 greenhouse gas balance in an Atlantic peat bog, *Biogeosciences*, 10, 1067–1082, <https://doi.org/10.5194/bg-10-1067-2013>,
537 2013.

538 Berhongaray, G., Verlinden, M. S., Broeckx, L. S., Janssens, I. A., and Ceulemans, R.: Soil carbon and belowground carbon
539 balance of a short-rotation coppice: assessments from three different approaches, *GCB Bioenergy*, 9, 299–313,
540 <https://doi.org/10.1111/gcbb.12369>, 2017.

541 Bianchi, A., Larmola, T., Kekkonen, H., Saarnio, S., and Lang, K.: Review of Greenhouse Gas Emissions from Rewetted
542 Agricultural Soils, *WETLANDS*, 41, 108, <https://doi.org/10.1007/s13157-021-01507-5>, 2021.

543 Bockermann, C., Eickenscheidt, T., and Droesler, M.: Adaptation of fen peatlands to climate change: rewetting and
544 management shift can reduce greenhouse gas emissions and offset climate warming effects, *BIOGEOCHEMISTRY*,
545 <https://doi.org/10.1007/s10533-023-01113-z>, 2024.

546 Boonman, C. C. F., Heuts, T. S., Vroom, R. J. E., Geurts, J. J. M., and Fritz, C.: Wetland plant development overrides
547 nitrogen effects on initial methane emissions after peat rewetting, *Aquat. Bot.*, 184, 103598,
548 <https://doi.org/10.1016/j.aquabot.2022.103598>, 2023.

549 Delegido, J., Verrelst, J., Rivera, J. P., Ruiz-Verdú, A., and Moreno, J.: Brown and *green* LAI mapping through spectral
550 indices, *Int. J. Appl. Earth Obs. Geoinformation*, 35, 350–358, <https://doi.org/10.1016/j.jag.2014.10.001>, 2015.

551 Dobbie, K. E., McTaggart, I. P., and Smith, K. A.: Nitrous oxide emissions from intensive agricultural systems: Variations
552 between crops and seasons, key driving variables, and mean emission factors, *J. Geophys. Res. Atmospheres*, 104, 26891–
553 26899, <https://doi.org/10.1029/1999JD900378>, 1999.

554 Duan, Y., Guo, B., Zhang, L., Li, J., Li, S., Zhao, W., Yang, G., Zhou, S., Zhou, C., Song, P., Li, P., Fang, L., Hou, S., Shi,
555 D., Zhao, H., and Guo, P.: Interactive climate-soil forces shape the spatial distribution of foliar N:P stoichiometry in
556 *Vaccinium uliginosum* planted in agroforests of Northeast China, *Front. Ecol. Evol.*, 10,
557 <https://doi.org/10.3389/fevo.2022.1065680>, 2022.

- 558 Eposito, D., Overall, J., and Grace, M. H.: Alaskan Berry Extracts Promote Dermal Wound Repair Through Modulation of
559 Bioenergetics and Integrin Signaling, *Front. Pharmacol.*, 10, <https://doi.org/10.3389/fphar.2019.01058>, 2019.
- 560 Evans, C. D., Peacock, M., Baird, A. J., Artz, R. R. E., Burden, A., Callaghan, N., Chapman, P. J., Cooper, H. M., Coyle,
561 M., Craig, E., Cumming, A., Dixon, S., Gauci, V., Grayson, R. P., Helfter, C., Heppell, C. M., Holden, J., Jones, D. L.,
562 Kaduk, J., Levy, P., Matthews, R., McNamara, N. P., Misselbrook, T., Oakley, S., Page, S. E., Rayment, M., Ridley, L. M.,
563 Stanley, K. M., Williamson, J. L., Worrall, F., and Morrison, R.: Overriding water table control on managed peatland
564 greenhouse gas emissions, *Nature*, <https://doi.org/10.1038/s41586-021-03523-1>, 2021.
- 565 FMI 2024. Finnish Meteorological Institute open data on weather monitoring. Available at:
566 <https://opendata.fmi.fi/wfs?request=GetCapabilities>
- 567 Freeman, B. W. J., Evans, C. D., Musarika, S., Morrison, R., Newman, T. R., Page, S. E., Wiggs, G. F. S., Bell, N. G. A.,
568 Styles, D., Wen, Y., Chadwick, D. R., and Jones, D. L.: Responsible agriculture must adapt to the wetland character of mid-
569 latitude peatlands, *Glob. Change Biol.*, 28, 3795–3811, <https://doi.org/10.1111/gcb.16152>, 2022.
- 570 Gregersen, P. L., Culetic, A., Boschian, L., and Krupinska, K.: Plant senescence and crop productivity, *Plant Mol. Biol.*, 82,
571 603–622, <https://doi.org/10.1007/s11103-013-0013-8>, 2013. Guenther, A., Barthelmes, A., Huth, V., Joosten, H., Jurasinski,
572 G., Koebisch, F., and Couwenberg, J.: Prompt rewetting of drained peatlands reduces climate warming despite methane
573 emissions, *Nat. Commun.*, 11, 1644–1644, <https://doi.org/10.1038/s41467-020-15499-z>, 2020.
- 574 Harris, Z. M., Alberti, G., Viger, M., Jenkins, J. R., Rowe, R., McNamara, N. P., and Taylor, G.: Land-use change to
575 bioenergy: grassland to short rotation coppice willow has an improved carbon balance, *GCB Bioenergy*, 9, 469–484,
576 <https://doi.org/10.1111/gcbb.12347>, 2017.
- 577 Hiraishi, T., Krug, T., Tanabe, K., Srivastava, N., Baasansuren, J., Fukuda, M., and Troxler, T. G.: Supplement to the 2006
578 IPCC guidelines for national greenhouse gas inventories: Wetlands, IPCC, Switzerland, 2014.
- 579 Honkanen, H., Kekkonen, H., Heikkinen, J., Kaseva, J., and Lång, K.: Minor effects of no-till treatment on GHG emissions
580 of boreal cultivated peat soil, *Biogeochemistry*, <https://doi.org/10.1007/s10533-023-01097-w>, 2023.
- 581 Huang, Y., Ciais, P., Luo, Y., Zhu, D., Wang, Y., Qiu, C., Goll, D. S., Guenet, B., Makowski, D., De Graaf, I., Leifeld, J.,
582 Kwon, M. J., Hu, J., and Qu, L.: Tradeoff of CO₂ and CH₄ emissions from global peatlands under water-table drawdown,
583 *Nat. Clim. Change*, 11, 618–622, <https://doi.org/10.1038/s41558-021-01059-w>, 2021.
- 584 Humpenöder, F., Karstens, K., Lotze-Campen, H., Leifeld, J., Menichetti, L., Barthelmes, A., and Popp, A.: Peatland
585 protection and restoration are key for climate change mitigation, *Environ. Res. Lett.*, 15, 104093,
586 <https://doi.org/10.1088/1748-9326/abae2a>, 2020.
- 587 Jacquemart, A.-L.: *Vaccinium Uliginosum* L., *J. Ecol.*, 84, 771–785, <https://doi.org/10.2307/2261339>, 1996.
- 588 Jokinen, P., Pirinen, P., Kaukoranta, J.-P., Kangas, A., Alenius, P., Eriksson, P., Johansson, M., and Wilkman, S.: Tilastoja
589 Suomen ilmastosta ja merestä 1991-2020, Ilmatieteen laitos, 2021.
- 590 Kandel, T. P., Elsgaard, L., and Laerke, P. E.: Measurement and modelling of CO₂ flux from a drained fen peatland
591 cultivated with reed canary grass and spring barley, *Glob. Change Biol. Bioenergy*, 5, 548–561,
592 <https://doi.org/10.1111/gcbb.12020>, 2013.
- 593 Kandel, T. P., Karki, S., Elsgaard, L., Labouriau, R., and Laerke, P. E.: Methane fluxes from a rewetted agricultural fen
594 during two initial years of paludiculture, *Sci. Total Environ.*, 713, 136670–136670,
595 <https://doi.org/10.1016/j.scitotenv.2020.136670>, 2020.
- 596 Karki, S., Elsgaard, L., Audet, J., and Laerke, P. E.: Mitigation of greenhouse gas emissions from reed canary grass in
597 paludiculture: effect of groundwater level, *Plant Soil*, 383, 217–230, <https://doi.org/10.1007/s11104-014-2164-z>, 2014.
- 598 Kasimir, Å., He, H., Coria, J., and Nordén, A.: Land use of drained peatlands: Greenhouse gas fluxes, plant production, and
599 economics, *Glob. Change Biol.*, 24, 3302–3316, <https://doi.org/10.1111/gcb.13931>, 2018.
- 600 Keck, H., Meurer, K. H. E., Jordan, S., Kätterer, T., Hadden, D., and Grelle, A.: Setting-aside cropland did not reduce
601 greenhouse gas emissions from a drained peat soil in Sweden, *Front. Environ. Sci.*, 12,
602 <https://doi.org/10.3389/fenvs.2024.1386134>, 2024.

- 603 Kutzbach, L., Schneider, J., Sachs, T., Giebels, M., Nykanen, H., Shurpali, N. J., Martikainen, P. J., Alm, J., and Wilmking,
604 M.: CO₂ flux determination by closed-chamber methods can be seriously biased by inappropriate application of linear
605 regression, *Biogeosciences*, 4, 1005–1025, <https://doi.org/10.5194/bg-4-1005-2007>, 2007.
- 606 Lammirato, C., Wallman, M., Weslien, P., Klemetsson, L., and Rütting, T.: Measuring frequency and accuracy of annual
607 nitrous oxide emission estimates, *Agric. For. Meteorol.*, 310, 108624, <https://doi.org/10.1016/j.agrformet.2021.108624>,
608 2021.
- 609 Lätti, A. K., Jaakola, L., Riihinen, K. R., and Kainulainen, P. S.: Anthocyanin and Flavonol Variation in Bog Bilberries
610 (*Vaccinium uliginosum* L.) in Finland, *J. Agric. Food Chem.*, 58, 427–433, <https://doi.org/10.1021/jf903033m>, 2010.
- 611 Lehtonen, H., Huan-Niemi, E., and Niemi, J.: The transition of agriculture to low carbon pathways with regional
612 distributive impacts, *Environ. Innov. Soc. Transit.*, 44, 1–13, <https://doi.org/10.1016/j.eist.2022.05.002>, 2022.
- 613 Leifeld, J. and Menichetti, L.: The underappreciated potential of peatlands in global climate change mitigation strategies,
614 *Nat. Commun.*, 9, 1071–1071, <https://doi.org/10.1038/s41467-018-03406-6>, 2018.
- 615 Leppelt, T., Dechow, R., Gebbert, S., Freibauer, A., Lohila, A., Augustin, J., Droesler, M., Fiedler, S., Glatzel, S., Hoepfer,
616 H., Jaerveoja, J., Laerke, P. E., Maljanen, M., Mander, U., Maekiranta, P., Minkkinen, K., Ojanen, P., Regina, K., and
617 Stromgren, M.: Nitrous oxide emission budgets and land-use-driven hotspots for organic soils in Europe, *Biogeosciences*,
618 11, 6595–6612, <https://doi.org/10.5194/bg-11-6595-2014>, 2014.
- 619 Liu, W., Fritz, C., Van Belle, J., and Nonhebel, S.: Production in peatlands: Comparing ecosystem services of different land
620 use options following conventional farming, *Sci. Total Environ.*, 875, 162534,
621 <https://doi.org/10.1016/j.scitotenv.2023.162534>, 2023.
- 622 LLOYD, J. and TAYLOR, J.: On the Temperature-Dependence of Soil Respiration, *Funct. Ecol.*, 8, 315–323,
623 <https://doi.org/10.2307/2389824>, 1994.
- 624 Lohila, A., Aurela, M., Regina, K., and Laurila, T.: Soil and total ecosystem respiration in agricultural fields: effect of soil
625 and crop type, *Plant Soil*, 251, 303–317, <https://doi.org/10.1023/A:1023004205844>, 2003.
- 626 Lohila, A., Aurela, M., Tuovinen, J., and Laurila, T.: Annual CO₂ exchange of a peat field growing spring barley or
627 perennial forage grass, *J. Geophys. Res.-Atmospheres*, 109, D18116–D18116, <https://doi.org/10.1029/2004JD004715>,
628 2004.
- 629 Long, S. P. and Hällgren, J.-E.: Measurement of CO₂ assimilation by plants in the field and the laboratory, in:
630 *Photosynthesis and Production in a Changing Environment: A field and laboratory manual*, edited by: Hall, D. O., Scurlock,
631 J. M. O., Bolhàr-Nordenkamp, H. R., Leegood, R. C., and Long, S. P., Springer Netherlands, Dordrecht, 129–167,
632 https://doi.org/10.1007/978-94-011-1566-7_9, 1993.
- 633 Maljanen, M., Liikanen, A., Silvola, J., and Martikainen, P.: Measuring N₂O emissions from organic soils by closed
634 chamber or soil/snow N₂O gradient methods, *Eur. J. Soil Sci.*, 54, 625–631, <https://doi.org/10.1046/j.1365-2389.2003.00531.x>, 2003.
- 636 Maljanen, M., Hytonen, J., Makiranta, P., Alm, J., Minkkinen, K., Laine, J., and Martikainen, P. J.: Greenhouse gas
637 emissions from cultivated and abandoned organic croplands in Finland, *Boreal Environ. Res.*, 12, 133–140, 2007.
- 638 Maljanen, M., Sigurdsson, B. D., Guomundsson, J., Oskarsson, H., Huttunen, J. T., and Martikainen, P. J.: Greenhouse gas
639 balances of managed peatlands in the Nordic countries - present knowledge and gaps, *Biogeosciences*, 7, 2711–2738,
640 <https://doi.org/10.5194/bg-7-2711-2010>, 2010.
- 641 Mander, U., Espenberg, M., Melling, L., and Kull, A.: Peatland restoration pathways to mitigate greenhouse gas emissions
642 and retain peat carbon, *BIOGEOCHEMISTRY*, <https://doi.org/10.1007/s10533-023-01103-1>, 2023.
- 643 Meek, D. W., Hatfield, J. L., Howell, T. A., Idso, S. B., and Reginato, R. J.: A Generalized Relationship between
644 Photosynthetically Active Radiation and Solar Radiation¹, *Agron. J.*, 76, 939–945,
645 <https://doi.org/10.2134/agronj1984.00021962007600060018x>, 1984.
- 646 Mitsch, W. J. and Wilson, R. F.: Improving the Success of Wetland Creation and Restoration with Know-How, Time, and
647 Self-Design, *Ecol. Appl.*, 6, 77–83, <https://doi.org/10.2307/2269554>, 1996.
- 648 Morrison, R., Rowe, R. L., Cooper, H. M., and McNamara, N. P.: Multi-year carbon budget of a mature commercial short
649 rotation coppice willow plantation, *GCB Bioenergy*, 11, 895–909, <https://doi.org/10.1111/gcbb.12608>, 2019.

- 650 Nielsen, C. K., Elsgaard, L., Jørgensen, U., and Lærke, P. E.: Soil greenhouse gas emissions from drained and rewetted
651 agricultural bare peat mesocosms are linked to geochemistry, *Sci. Total Environ.*, 896, 165083,
652 <https://doi.org/10.1016/j.scitotenv.2023.165083>, 2023.
- 653 Pacaldo, R. S., Volk, T. A., and Briggs, R. D.: Carbon Sequestration in Fine Roots and Foliage Biomass Offsets Soil CO₂
654 Effluxes along a 19-year Chronosequence of Shrub Willow (*Salix x dasyclados*) Biomass Crops, *BioEnergy Res.*, 7, 769–
655 776, <https://doi.org/10.1007/s12155-014-9416-x>, 2014.
- 656 Pasquet, S., Pellerin, S., and Poulin, M.: Three decades of vegetation changes in peatlands isolated in an agricultural
657 landscape, *Appl. Veg. Sci.*, 18, 220–229, <https://doi.org/10.1111/avsc.12142>, 2015.
- 658 Patrignani, A. and Ochsner, T. E.: Canopeo: A Powerful New Tool for Measuring Fractional Green Canopy Cover, *Agron.*
659 *J.*, 107, 2312–2320, <https://doi.org/10.2134/agronj15.0150>, 2015.
- 660 Raich, J. W., Rastetter, E. B., Melillo, J. M., Kicklighter, D. W., Steudler, P. A., Peterson, B. J., Grace, A. L., Moore III, B.,
661 and Vorosmarty, C. J.: Potential Net Primary Productivity in South America: Application of a Global Model, *Ecol. Appl.*, 1,
662 399–429, <https://doi.org/10.2307/1941899>, 1991.
- 663 Regina, K., Syvasalo, E., Hannukkala, A., and Esala, M.: Fluxes of N₂O from farmed peat soils in Finland, *Eur. J. Soil Sci.*,
664 55, 591–599, <https://doi.org/10.1111/j.1365-2389.2004.00622.x>, 2004.
- 665 Shepherd, M.J., Lindsey, L.E. and Lindsey, A.J. Soybean Canopy Cover Measured with Canopeo Compared with Light
666 Interception. *Agricultural & Environmental Letters* 3: 180031. doi:10.2134/aerl2018.06.0031, 2018.
- 667 Strack, M., Davidson, S. J., Hirano, T., and Dunn, C.: The Potential of Peatlands as Nature-Based Climate Solutions, *Curr.*
668 *Clim. Change Rep.*, 8, 71–82, <https://doi.org/10.1007/s40641-022-00183-9>, 2022.
- 669 Tanneberger, F., Birr, F., Couwenberg, J., Kaiser, M., Luthardt, V., Nerger, M., Pfister, S., Oppermann, R., Zeitz, J., Beyer,
670 C., van der Linden, S., Wichtmann, W., and Närmann, F.: Saving soil carbon, greenhouse gas emissions, biodiversity and
671 the economy: paludiculture as sustainable land use option in German fen peatlands, *Reg. Environ. Change*, 22, 69,
672 <https://doi.org/10.1007/s10113-022-01900-8>, 2022.
- 673 Viherä-Aarnio, A., Jyske, T., and Beuker, E.: Pajut biokiertoaloudessa - Materiaaleja, arvoaineita, ympäristöhyötyjä :
674 Synteesiraportti, Luonnonvarakeskus, 2022.
- 675 Vuorinen, J. and Mäkitie, O.: The method of soil testing in use in Finland, *Maatalouskoelaitoksen maatumkimusosasto*,
676 Helsinki, 44 pp., 1955.
- 677 Wilson, D., Blain, D., Couwenberg, J., Evans, C., Murdiyarso, D., Page, S., Renou-Wilson, F., Rieley, J., Strack, M., and
678 Tuittila, E.: Greenhouse gas emission factors associated with rewetting of organic soils, *Mires Peat*, 14, 1–28, 2016.
- 679 Zheng, D., Hunt, E., and Running, S.: A daily soil temperature model based on air temperature and precipitation for
680 continental applications, *Clim. Res.*, 2, 183–191, <https://doi.org/10.3354/cr002183>, 1993.
- 681